Structural Engineering and Mechanics, Vol. 43, No. 5 (2012) 691-709
DOI: http://dx.doi.org/10.12989/sem.2012.43.5.691

Investigation on deck-stay interaction of cable-stayed bridges with appropriate initial shapes

Ming-Yi Liu*, Li-Chin Lin and Pao-Hsii Wang

Department of Civil Engineering, Chung Yuan Christian University, Jhongli City, Taoyuan County 32023, Taiwan

(Received April 23, 2012, Revised August 8, 2012, Accepted August 9, 2012)

Abstract. This paper provides a variety of viewpoints to illustrate the mechanism of the deck-stay interaction with the appropriate initial shapes of cable-stayed bridges. Based on the smooth and convergent bridge shapes obtained by the initial shape analysis, the one-element cable system (OECS) and multi-element cable system (MECS) models of the Kao Ping Hsi Bridge in Taiwan are developed to verify the applicability of the analytical model and numerical formulation from the field observations in the authors' previous work. For this purpose, the modal analysis of the two finite element models are conducted to calculate the natural frequency and normalized mode shape of the individual modes of the bridge. The modal coupling assessment is also performed to obtain the generalized mass ratios among the structural components for each mode of the bridge. The findings indicate that the coupled modes are attributed to the frequency loci veering and mode localization when the "pure" deck-tower frequency and the "pure" stay cable frequency approach one another, implying that the mode shapes of such coupled modes are simply different from those of the deck-tower system or stay cables alone. The distribution of the generalized mass ratios between the deck-tower system and stay cables are useful indices for quantitatively assessing the degree of coupling for each mode. These results are demonstrated to fully understand the mechanism of the deck-stay interaction with the appropriate initial shapes of cable-stayed bridges.

Keywords: cable-stayed bridge; deck-stay interaction; initial shape analysis; one-element cable system; multi-element cable system

1. Introduction

In the last several decades, cable-stayed bridges have become popular due to their aesthetic appearance, structural efficiency, ease of construction and economic advantage. This type of bridge, however, is light and flexible, and has a low level of inherent damping. Consequently, they are susceptible to ambient excitations from wind, seismic and traffic loads. Since the geometric and dynamic properties of the bridges as well as the characteristics of the excitations are complex, it is necessary to fully understand the mechanism of the interaction among the structural components with reasonable bridge shapes, which is used to provide the essential information to accurately calculate the dynamic responses of the bridges under the complicated excitations.

*Corresponding author, Assistant Professor, E-mail: myliu@cycu.edu.tw

In the previous studies of bridge dynamics, the responses of a cable-stayed bridge can be categorized into global, local and coupled modes (Abdel-Ghaffar and Khalifa 1991). The global modes are primarily dominated by the deformations of the deck-tower system with the quasi-static motions of the stay cables; the local modes predominantly consist of the stay cable motions with negligible deformations of the deck-tower system; the coupled modes have substantial contributions from both the deck-tower system and stay cables. Since the towers are usually designed with a high rigidity to obtain an adequate efficiency of the system, the significant tower deformations do not occur in the lower modes sensitive to the ambient excitations (Gimsing 1997). Consequently, the coupled modes are considered to be dominated by the deck-stay interaction, while the contribution from the towers can be neglected. Numerical approaches based on the finite element method have been widely used to investigate the deck-stay interaction. The finite-element models of a cable-stayed bridge can be classified into two categories (Abdel-Ghaffar and Khalifa 1991): the one-element cable system (OECS), in which each stay cable is represented by a single cable element, and the multi-element cable system (MECS), in which each stay cable is discretized into multiple cable elements.

The deck-stay interaction has attracted much attention, because it not only significantly complicates both the natural frequency and mode shape characteristics of a cable-stayed bridge, but also potentially results in the large-amplitude stay cable vibrations even under the low-level deck oscillations. In the previous literature, the deck-stay interaction is due to the linear coupling (primary resonance) (Fujino *et al.* 1993, Warnitchai *et al.* 1993, 1995, Lilien and Pinto da Costa 1994, Pinto da Costa *et al.* 1996, Gattulli *et al.* 2002, Gattulli and Lepidi 2007) or the nonlinear coupling (secondary resonance), which can be further categorized into the subharmonic resonance of order 1/2 (two-to-one resonance) (Fujino *et al.* 1993, Warnitchai *et al.* 1993, 1995, Lilien and Pinto da Costa 1994, Pinto da Costa *et al.* 1996, Gattulli *et al.* 2002, Gattulli and Lepidi 2003) and the superharmonic resonance of order 2 (one-to-two resonance) (Lilien and Pinto da Costa 1994, Gattulli and Lepidi 2003, Gattulli *et al.* 2005). The primary, two-to-one and one-to-two resonances individually result in the fact that the global modes induce the direct, parametric and angle variation excitations of the local modes. Two types of simplified models: the single cable with moving anchorage (Warnitchai *et al*. 1995, Lilien and Pinto da Costa 1994, Pinto da Costa *et al.* 1996) and the cable-supported cantilever beam (Fujino *et al.* 1993, Warnitchai *et al.* 1993, Gattulli *et al.* 2002, Gattulli and Lepidi 2003, Gattulli *et al.* 2005, Gattulli and Lepidi 2007), have been presented to theoretically investigate the deck-stay interaction. To extend the results of the simplified models, the OECS and MECS models of full cable-stayed bridges based on the finite element method have been widely used to explore such coupled phenomena of real structures (Abdel-Ghaffar and Khalifa 1991, Gattulli and Lepidi 2007, Tuladhar *et al.* 1995, Caetano *et al.* 2000a, b, Au *et al.* 2001, Caetano *et al.* 2008). By focusing on the analytical and numerical study of the linear coupling, the localization factor was introduced to reveal the frequency veering phenomenon and to evaluate the mode hybridization level of a cable-stayed bridge (Gattulli and Lepidi 2007). On the basis of this research, the ambient vibration measurements were conducted to investigate the deck-stay interaction. It was suggested that the nonlinear coupling is not consistent with the measurement data. In contrast, the linear coupling is recognized as the critical excitation source of the coupled modes (Caetano *et al.* 2008).

In parallel to the previous work (Gattulli and Lepidi 2007, Caetano *et al.* 2008), the authors of the present paper also studied the deck-stay interaction of cable-stayed bridges based on the analytical and numerical methods as well as the long-term comprehensive full-scale measurements (Liu *et al.* 2005). The measurement data indicated that the deck oscillations of small to moderate amplitudes

are coupled with the large-amplitude stay cable vibrations due to the linear coupling between these two components. An analytical model of the single cable with spring-mass oscillator was presented to explain such mechanism attributed to the frequency loci veering and mode localization. Furthermore, the "pure" deck modes, "pure" cable modes and coupled modes are successfully captured by the proposed model. These phenomena are verified by the numerical simulations of the OECS and MECS models of a full cable-stayed bridge. The concepts of the indices for quantitatively assessing the degree of coupling among the structural components were also appeared in this research.

It is important to investigate the deck-stay interaction with the appropriate initial shape of a cable-stayed bridge. This is because such initial shape not only reasonably provides the geometric configuration as well as the prestress distribution of the bridge under the weight of the deck-tower system and the pretension forces in the stay cables, but also definitely ensures the satisfaction of the relations for the equilibrium conditions, boundary conditions and architectural design requirements (Wang *et al.* 1993, Wang and Yang 1996, Wang *et al*. 2002, 2004). The computational procedures for the initial shape analysis of the OECS and MECS models were presented for this reason (Wang *et al.* 2010, Liu *et al.* 2011). However, few researchers have studied the deck-stay interaction considering the initial shape effect.

The objective of this paper is to fully understand the mechanism of the deck-stay interaction with the appropriate initial shapes of cable-stayed bridges. Based on the smooth and convergent bridge shapes obtained by the initial shape analysis (Wang *et al.* 2010, Liu *et al.* 2011), the OECS and MECS models of the Kao Ping Hsi Bridge in Taiwan are developed to verify the applicability of the analytical model and numerical formulation from the field observations (Liu *et al*. 2005). For this purpose, the modal analysis of the two finite element models are conducted to calculate the natural frequency and normalized mode shape of the individual modes of the bridge. The modal coupling assessment is also performed to obtain the generalized mass ratios among the structural components for each mode of the bridge. These results can be used to provide a variety of viewpoints to illustrate the mechanism of the deck-stay interaction with the appropriate initial shapes of cable-stayed bridges.

2. Finite element formulation

On the basis of the finite element concepts, a cable-stayed bridge can be considered as an assembly of a finite number of cable elements for the stay cables and beam-column elements for both the decks and towers. Several assumptions are adopted in this study: the material is homogeneous and isotropic; the stress-strain relationship of the material remains within the linear elastic range during the whole nonlinear response; the external forces are displacement independent; large displacements and large rotations are allowed, but strains are small; each stay cable is fixed to both the deck and tower at their joints of attachment. Based on the system equations with the consideration of geometric nonlinearities, the initial shape analysis, modal analysis and modal coupling assessment of cable-stayed bridges are conducted in this research.

2.1 Geometric nonlinearities

To reasonably simulate cable-stayed bridges, three types of geometric nonlinearities: the cable sag,

beam-column and large displacement effects, are considered in this study.

A stay cable will sag into a catenary shape due to its weight and tensile force. Such cable sag effect has to be taken into consideration when the stay cable is represented by a single straight cable element. A stay cable with tensile stiffness is assumed to be perfectly elastic. The compressive, shear and bending stiffnesses of the stay cable are negligible. The cable sag nonlinearity can be simulated based on the equivalent modulus of elasticity of the stay cable (Ernst 1965)

$$E_{eq} = \frac{E_c}{1 + \frac{(wl_c)^2 A_c E_c}{12T^3}} \tag{1}$$

where E_c, A_c and l_c are the effective modulus of elasticity, the cross-sectional area and the horizontal projected length of the stay cable, respectively; w is the weight of the stay cable per unit length; T is the tension in the stay cable. The stiffness matrix of a cable element in Fig. 1 can be expressed as

$$KE_{jk} = \begin{cases} \left[\frac{E_{eq}A_c}{L_c}\right] & u_1 > 0 \\ [0] & u_1 \le 0 \end{cases} \tag{2}$$

where u_1 is the element coordinate for the relative axial deformation; L_c is the chord length of the

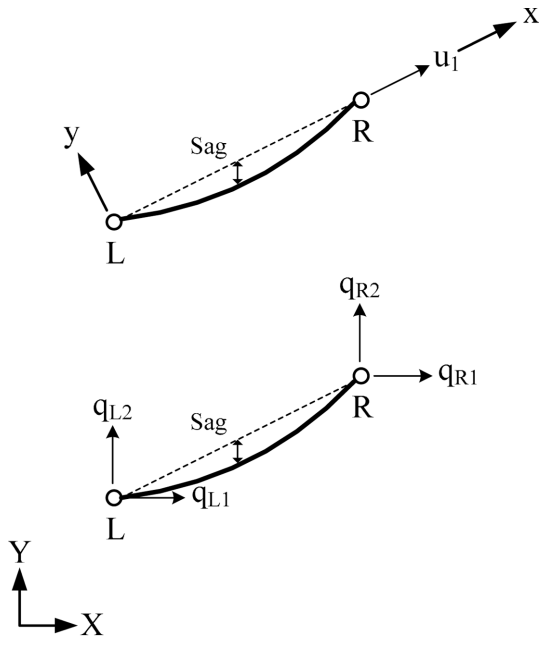

Fig. 1 Cable element for simulating the stiffness of each stay cable

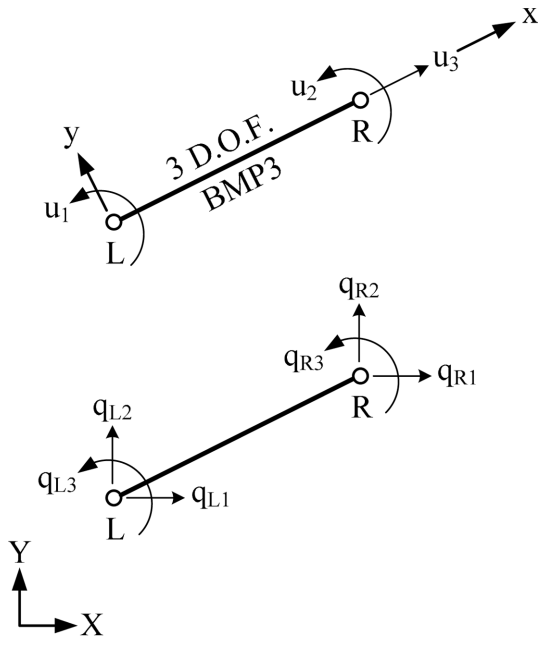

Fig. 2 Beam-column element for simulating the stiffness of each deck and tower

stay cable.

High pretension forces in the stay cables can result in large compressive forces in the deck-tower system of a cable-stayed bridge. For this reason, the beam-column effect between such compressive forces and bending moments has to be considered when beam-column elements are used to simulate both the decks and towers. For a beam-column element based on the Euler-Bernoulli beam theory in Fig. 2, shear strains of the element can be neglected. u_1, u_2 and u_3 are the element coordinates for the left end rotation, the right end rotation and the relative axial deformation, respectively. The stiffness matrix of the beam-column element can be written as

$$KE_{jk} = \frac{E_b I_b}{L_b}\begin{bmatrix} C_s & C_t & 0 \\ C_t & C_s & 0 \\ 0 & 0 & R_t A_b / I_b \end{bmatrix} \tag{3}$$

where E_b, A_b, I_b and L_b are the modulus of elasticity, the cross-sectional area, the moment of inertia and the length of the beam-column element, respectively; C_s, C_t and R_t are the stability functions representing the interaction between the axial and bending stiffnesses of the beam-column element (Fleming 1979).

In general, large displacements occur in the deck-tower system due to the large span and less weight of a cable-stayed bridge. Such effect has to be taken into consideration when the equilibrium equations are derived from the deformed position. Under these conditions, the element coordinate u_j can be expressed as a nonlinear function of the system coordinate q_α in both Fig. 1 and Fig. 2, i.e., $u_j = u_j(q_\alpha)$. By differentiating u_j with respect to q_α, the first-order and second-order coordinate transformation coefficients can be individually written as

$$a_{j\alpha} = \frac{\partial u_j}{\partial q_\alpha} \tag{4}$$

$$a_{j\alpha,\beta} = \frac{\partial a_{j\alpha}}{\partial q_\beta} = \frac{\partial^2 u_j}{\partial q_\alpha \partial q_\beta} \tag{5}$$

$a_{j\alpha}$ and $a_{j\alpha,\beta}$ for the stiffness matrices of the cable and beam-column elements can be found in Wang *et al.* (1993), which are provided to develop the system tangential stiffness matrix in Section 2.2.

In addition to the element stiffness matrices, the element mass matrices are introduced to fully understand the essential properties of a cable-stayed bridge. Based on the consistent mass model, the mass distribution of each stay cable and that of each deck and tower can be simulated by a cable element and a beam-column element, respectively. The mass matrix of the former with four element coordinates u_j $(j = 1-4)$ in Fig. 3 and that of the latter with six element coordinates u_j $(j = 1-6)$ in Fig. 4 can be individually expressed as

$$ME_{jk} = \frac{\rho_c A_c L_c}{6}\begin{bmatrix} 2 & 0 & 1 & 0 \\ 0 & 2 & 0 & 1 \\ 1 & 0 & 2 & 0 \\ 0 & 1 & 0 & 2 \end{bmatrix} \tag{6}$$

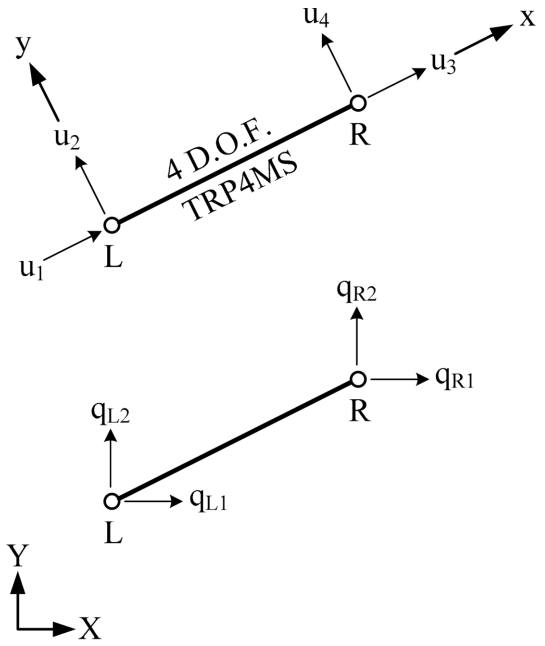

u_j : Element Coordinates
q_α : System Coordinates
x, y : Local Coordinate System
X, Y: Global Coordinate System

Fig. 3 Cable element for simulating the mass of each stay cable

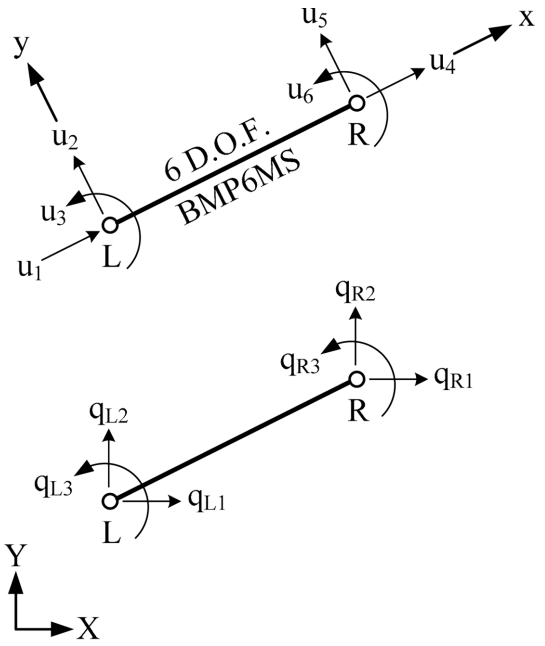

u_j : Element Coordinates
q_α : System Coordinates
x, y : Local Coordinate System
X, Y: Global Coordinate System

Fig. 4 Beam-column element for simulating the mass of each deck and tower

$$ME_{jk} = \frac{\rho_b A_b L_b}{420}\begin{bmatrix} 140 & 0 & 0 & 70 & 0 & 0 \\ 0 & 156 & 22L_b & 0 & 54 & -13L_b \\ 0 & 22L_b & 4L_b^2 & 0 & 13L_b & -3L_b^2 \\ 70 & 0 & 0 & 140 & 0 & 0 \\ 0 & 54 & 13L_b & 0 & 156 & -22L_b \\ 0 & -13L_b & -3L_b^2 & 0 & -22L_b & 4L_b^2 \end{bmatrix} \tag{7}$$

where ρ_c and ρ_b are the mass densities of the cable and beam-column elements, respectively. The coordinate transformation coefficient $a'_{j\alpha}$ connecting u_j and q_α for the mass matrices of the cable and beam-column elements can be found in Wang *et al*. (2002).

2.2 System equations

The system equations in generalized coordinates of a nonlinear finite element model of a cable-stayed bridge can be derived from Lagrange's virtual work principle

$$M_{\alpha\beta}\ddot{q}_{\beta}+D_{\alpha\beta}\dot{q}_{\beta}+\sum_{EL}S_j a_{j\alpha}=P_{\alpha},\quad \alpha=1,2,3,\ldots,N \tag{8}$$

$$M_{\alpha\beta}=\sum_{EL}ME_{jk}a'_{j\alpha}a'_{k\beta} \tag{9}$$

$$S_j=KE_{jk}u_k+S_j^0 \tag{10}$$

$$P_{\alpha}=\vec{\overrightarrow{K}}^{j}\cdot\vec{\overrightarrow{b}}^{j}_{\alpha} \tag{11}$$

$$\vec{\overrightarrow{b}}^{j}_{\alpha}=\frac{\partial\vec{\overrightarrow{W}}^{j}}{\partial q_{\alpha}} \tag{12}$$

$$\dot{q}_{\alpha}=\frac{dq_{\alpha}}{dt} \tag{13}$$

$$\ddot{q}_{\alpha}=\frac{d^2q_{\alpha}}{dt^2} \tag{14}$$

where $M_{\alpha\beta}$ and $D_{\alpha\beta}$ are the system mass and damping matrices, respectively, which both are assumed to be constant; S_j is the element force vector; P_{α} is the external force vector; S_j^0 is the initial element force vector; $\vec{\overrightarrow{K}}^{j}$ is the external nodal force vector; $\vec{\overrightarrow{b}}^{j}_{\alpha}$ is the basis vector; $\vec{\overrightarrow{W}}^{j}$ is the displacement vector corresponding to $\vec{\overrightarrow{K}}^{j}$; $\dot{q}_{\alpha}$ and $\ddot{q}_{\alpha}$ are the system velocity and acceleration vectors, respectively; t is the time; N is the number of degrees of freedom; the subscripts α and β denote the numbers of the system coordinates; the subscripts j and k represent the numbers of the element coordinates; the superscript j denotes the nodal number; Σ_{EL} represents the summation over all elements.

Considering of three types of geometric nonlinearities mentioned in Section 2.1, KE_{jk} of a cable element and that of a beam-column element can be individually obtained from Eq. (2) and Eq. (3). The former and the latter are due to the cable sag effect and the beam-column effect, respectively. Similarly, ME_{jk} of the cable element and that of the beam-column element can be individually obtained from Eq. (6) and Eq. (7). $u_j, a_{j\alpha}$ and $\vec{\overrightarrow{b}}^{j}_{\alpha}$ are nonlinear functions of q_{α} when large displacements occur. $\vec{\overrightarrow{K}}^{j}$ can be written as a function of q_{α} if they are displacement dependent forces. $M_{\alpha\beta}$ and $D_{\alpha\beta}$ are both assumed to be constant, because only nonlinearities in stiffness are considered in this system.

Eq. (8) is a set of simultaneous second-order nonlinear ordinary differential equations. In order to incrementally solve these equations, the linearized system equations in a small time (or force) interval are derived based on the first-order Taylor series expansion of Eq. (8)

$$M_{\alpha\beta}\Delta\ddot{q}^{n}_{\beta}+D_{\alpha\beta}\Delta\dot{q}^{n}_{\beta}+{}^{2}K^{n}_{\alpha\beta}\Delta q^{n}_{\beta}={}_{u}P^{n}_{\alpha}+\Delta P^{n}_{\alpha},\quad t^n\le t\le t^n+\Delta t^n \tag{15}$$

$${}^{2}K^{n}_{\alpha\beta}=\sum_{EL}KE^{n}_{jk}a^{n}_{j\alpha}a^{n}_{k\beta}+\sum_{EL}S^{n}_{j}a^{n}_{j\alpha,\beta}-{}^{n}\vec{\overrightarrow{K}}^{j}\cdot{}^{n}\vec{\overrightarrow{b}}^{j}_{\alpha,\beta}-{}^{n}\vec{\overrightarrow{K}}^{j}_{\beta}\cdot{}^{n}\vec{\overrightarrow{b}}^{j}_{\alpha} \tag{16}$$

$$\vec{\overrightarrow{b}}^{j}_{\alpha,\beta}=\frac{\partial\vec{\overrightarrow{b}}^{j}_{\alpha}}{\partial q_{\beta}} \tag{17}$$

$$\vec{K}_{\alpha}^{j} = \frac{\partial \vec{R}^{j}}{\partial q_{\alpha}} \tag{18}$$

$${}_{u}P_{\alpha}^{n} = P_{\alpha}^{n} - M_{\alpha\beta}\ddot{q}_{\beta}^{n} - D_{\alpha\beta}\dot{q}_{\beta}^{n} - \sum_{EL} S_{j}^{n} a_{j\alpha}^{n} \tag{19}$$

$$\Delta P_{\alpha}^{n} = P_{\alpha}^{n+1} - P_{\alpha}^{n} \tag{20}$$

$$\Delta q_{\alpha}^{n} = q_{\alpha}^{n+1} - q_{\alpha}^{n} \tag{21}$$

$$\Delta \dot{q}_{\alpha}^{n} = \dot{q}_{\alpha}^{n+1} - \dot{q}_{\alpha}^{n} \tag{22}$$

$$\Delta \ddot{q}_{\alpha}^{n} = \ddot{q}_{\alpha}^{n+1} - \ddot{q}_{\alpha}^{n} \tag{23}$$

$$\Delta t^{n} = t^{n+1} - t^{n} \tag{24}$$

where ${}^{2}K_{\alpha\beta}^{n}$ is the system tangential stiffness matrix; ${}_{u}P_{\alpha}^{n}$ is the unbalanced force vector; ΔP_{α}^{n} is the incremental external force vector; $\Delta q_{\alpha}^{n}, \Delta \dot{q}_{\alpha}^{n}$ and $\Delta \ddot{q}_{\alpha}^{n}$ are the incremental system coordinate, velocity and acceleration vectors, respectively; Δt^{n} is the time increment; the superscripts n and $n+1$ denote the numbers of the time (or force) steps; the superscript 2 represents the second-order iteration matrix.

${}^{2}K_{\alpha\beta}^{n}$ in Eq. (16) consists of four terms. The first term is the elastic stiffness matrix, while the second and third terms are the geometric stiffness matrices induced by large displacements. Furthermore, the fourth term is the geometric stiffness matrix induced by displacement dependent forces, which is neglected in this study.

Eq. (15) is a set of simultaneous second-order linear ordinary differential equations in a small time interval, which can be solved by the direct integration method (Wang *et al.* 2002).

2.3 Initial shape analysis

The initial shape of a cable-stayed bridge provides the geometric configuration as well as the prestress distribution of such bridge under the weight of the deck-tower system and the pretension forces in the stay cables. The relations for the equilibrium conditions, boundary conditions and architectural design requirements should be satisfied. Considering of three types of geometric nonlinearities, i.e., the cable sag, beam-column and large displacement effects, the initial shape analysis of the OECS and MECS models are presented in this study.

For the initial shape analysis of the OECS model, the weight of the deck-tower system is considered, whereas the weight of the stay cables is neglected. The shape finding computation is performed using a two-loop iteration method: an equilibrium iteration and a shape iteration (Wang *et al.* 1993, Wang and Yang 1996, Wang *et al.* 2002, 2004, 2010, Liu *et al*. 2011). It can be started with an estimated initial element force (pretension force) in the stay cables. Based on the reference configuration (architectural design form) with no deflection and zero prestress in the deck-tower system, the equilibrium of the whole bridge under the weight of the deck-tower system can be first determined by incrementally solving the linearized system equations

$$ {}^{2}K^{n}_{\alpha\beta}\Delta q^{n}_{\beta} = {}_{u}P^{n}_{\alpha} + \Delta P^{n}_{\alpha},\ P^{n}_{\alpha} \le P_{\alpha} \le P^{n+1}_{\alpha} \tag{25} $$

$$ {}_{u}P^{n}_{\alpha} = P^{n}_{\alpha} - \sum_{EL} S^{n}_{j} a^{n}_{j\alpha} \tag{26} $$

which are individually derived from Eq. (15) and Eq. (19) with negligible inertial and damping effects due to the static case. On the basis of Eq. (25) and Eq. (26), the equilibrium iteration is performed using the Newton-Raphson method (Wang *et al.* 1993, Wang and Yang 1996, Wang *et al.* 2002, 2004, 2010, Liu *et al.* 2011).

After the above equilibrium iteration, the bridge configuration satisfies the equilibrium and boundary conditions, however, the architectural design requirements are, in general, not fulfilled. This is because large displacements and variable bending moments occur in the deck-tower system due to the large bridge span. Under these conditions, the shape iteration is conducted to reduce the displacements and to smoothen the bending moments, and the appropriate initial shape can therefore be obtained.

A number of control points are selected for insuring that both the deck and tower displacements satisfy the architectural design requirements in the shape iteration

$$ \left| \frac{q_{\alpha}}{L_{r}} \right| \le \varepsilon_{r} \tag{27} $$

where q_{α} is the displacement in a certain direction of the control point; L_r is the reference length; ε_r is the convergence tolerance. For checking the deck displacement, each control point is the node intersected by the deck and the stay cable. q_{α} and L_r individually denote the vertical displacement of the control point and the main span length. Similarly, each node intersected by the tower and the stay cable, or located on the top of the tower is chosen as the control point for checking the tower displacement. q_{α} and L_r represent the horizontal displacement of the control point and the tower height, respectively.

If Eq. (27) is not satisfied, the element axial forces calculated in the previous equilibrium iteration will be taken as the initial element forces in the new equilibrium iteration, and the corresponding equilibrium of the whole bridge under the weight of the deck-tower system will be determined again. The shape iteration will then be repeated until Eq. (27) is satisfied. Under these conditions, the convergent configuration can be found and used as the initial shape of the OECS model.

The initial shape analysis of the MECS model is also performed to reasonably simulate the bridge configuration. Based on the initial shape of the OECS model obtained previously, the both end coordinates and pretension force in each single stay cable can be used for the shape finding computation of the corresponding stay cable discretized into multiple elements using the catenary function method (Wang *et al.* 2010, Liu *et al.* 2011). Incorporating the interior nodal coordinates and pretension forces in each discrete stay cable into the bridge model, and then conducting the two-loop iteration method again, the convergent configuration can be found and used as the initial shape of the MECS model.

2.4 Modal analysis

Under the assumption that the system vibrates with a small amplitude around a certain nonlinear static state, in which the variation in such state induced by the vibration is negligible, the modal

analysis of a cable-stayed bridge can be conducted based on the linearized system equation

$$M^A_{\alpha\beta}\ddot{q}_\beta + {}^2K^A_{\alpha\beta}q_\beta = 0 \tag{28}$$

where $M^A_{\alpha\beta}$ and ${}^2K^A_{\alpha\beta}$ are the system mass and system tangential stiffness matrices with respect to the nonlinear static state q^A_α, respectively. The initial shape obtained in Section 2.3 can be regarded as q^A_α. Eq. (28) is derived from Eq. (15) with negligible damping and force effects. On the basis of Eq. (28) representing the free vibration of the undamped system, the natural frequency f_n and the normalized mode shape $\overline{Y}_n$ of the nth mode can be calculated by the subspace iteration method (Wang *et al.* 2002).

2.5 Modal coupling assessment

According to the results of both the initial shape analysis (Section 2.3) and modal analysis (Section 2.4) with the consideration of geometric nonlinearities (Section 2.1) in the system equations (Section 2.2), three indices for quantitatively assessing the degree of coupling among the stay cables, decks and towers of a cable-stayed bridge in each mode are presented as

$$\overline{M}^s_n = \frac{(\overline{Y}^s_n)^T M^s \overline{Y}^s_n}{(\overline{Y}^s_n)^T M^s \overline{Y}^s_n + (\overline{Y}^d_n)^T M^d \overline{Y}^d_n + (\overline{Y}^t_n)^T M^t \overline{Y}^t_n} \tag{29}$$

$$\overline{M}^d_n = \frac{(\overline{Y}^d_n)^T M^d \overline{Y}^d_n}{(\overline{Y}^s_n)^T M^s \overline{Y}^s_n + (\overline{Y}^d_n)^T M^d \overline{Y}^d_n + (\overline{Y}^t_n)^T M^t \overline{Y}^t_n} \tag{30}$$

$$\overline{M}^t_n = \frac{(\overline{Y}^t_n)^T M^t \overline{Y}^t_n}{(\overline{Y}^s_n)^T M^s \overline{Y}^s_n + (\overline{Y}^d_n)^T M^d \overline{Y}^d_n + (\overline{Y}^t_n)^T M^t \overline{Y}^t_n} \tag{31}$$

where $\overline{M}^j_n$ $(j = s, d, t)$ are the generalized mass ratios of the nth mode; M^j $(j = s, d, t)$ are the submatrices of $M^A_{\alpha\beta}$; $\overline{Y}^j_n$ $(j = s, d, t)$ are the subvectors of $\overline{Y}_n$ in the nth mode; the superscripts s, d and t denote the quantities of the stay cable, the deck and the tower, respectively. The sum of $\overline{M}^s_n$, $\overline{M}^d_n$ and $\overline{M}^t_n$ is 1 for the corresponding n.

3. Finite element models

To understand the deck-stay interaction with the appropriate initial shapes of cable-stayed bridges, an OECS model and a MECS model of the full Kao Ping Hsi Bridge are developed, as shown in Figs. 5(a) and 5(b), respectively. This bridge is an unsymmetrical single-deck cable-stayed bridge with a main span of 330 m and a side span of 184 m. The deck, which consists of steel box girders in the main span and concrete box girders in the side span, is supported by a total of 28 stay cables (S1-S28), arranged in a central plane originated at the 184 m tall, inverted Y-shaped, concrete tower. A more detailed description of the Kao Ping Hsi Bridge can be found in Cheng (2001).

Figs. 5(a) and 5(b) illustrate the two-dimensional finite element models of the bridge. The OECS and MECS models both contain 48 beam-column elements that simulate the deck and tower. For the

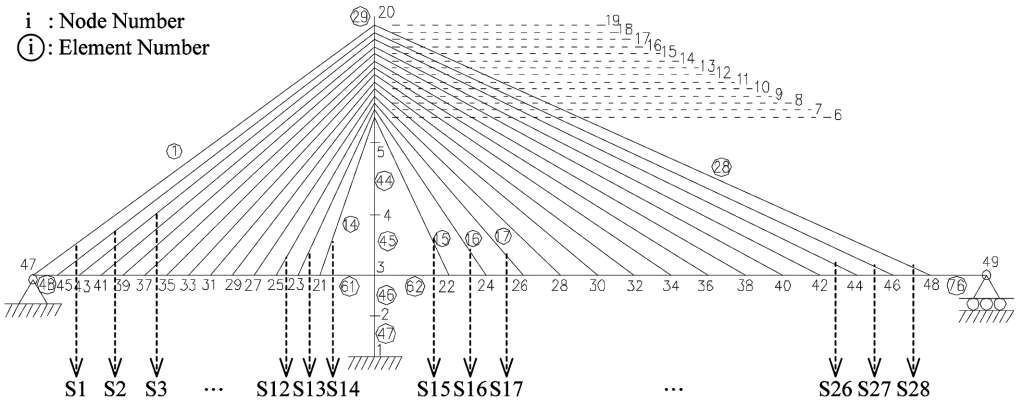

(a) OECS model

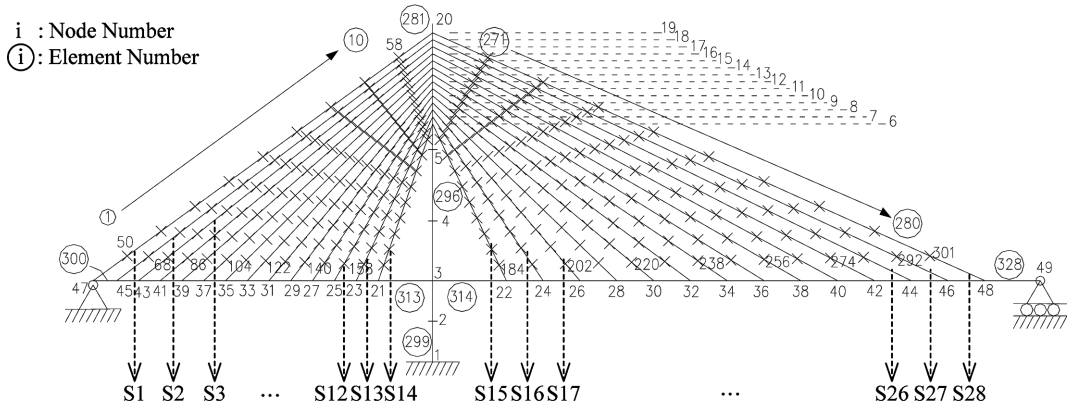

(b) MECS model

Fig. 5 Finite element models of the Kao Ping Hsi Bridge

MECS model, each stay cable is discretized into 10 cable elements, whereas a single cable element is used to simulate each stay cable in the OECS model. This fact indicates that the OECS and MECS models individually include 28 and 280 cable elements. Figs. 5(a) and 5(b) also show that 49 and 301 nodes are involved in the OECS and MECS models, respectively. A hinge, roller and fixed supports are used to model the boundary conditions of the left and right ends of the deck and the tower, respectively, and a rigid joint is employed to simulate the deck-tower connection. On the basis of the OECS and MECS models, the initial shape analysis, modal analysis and modal coupling assessment of the Kao Ping Hsi Bridge are conducted in this research.

4. Numerical results

Based on the OECS and MECS models of the Kao Ping Hsi Bridge developed in Section 3, the

initial shape analysis, modal analysis and modal coupling assessment are conducted using the finite element formulation presented in Section 2. The numerical results can be used to fully understand the mechanism of the deck-stay interaction with the appropriate initial shapes of cable-stayed bridges.

4.1 Initial shape analysis

Based on the finite element procedures presented in Section 2.3, the initial shape analysis of the OECS and MECS models are conducted to reasonably provide the geometric configuration of the

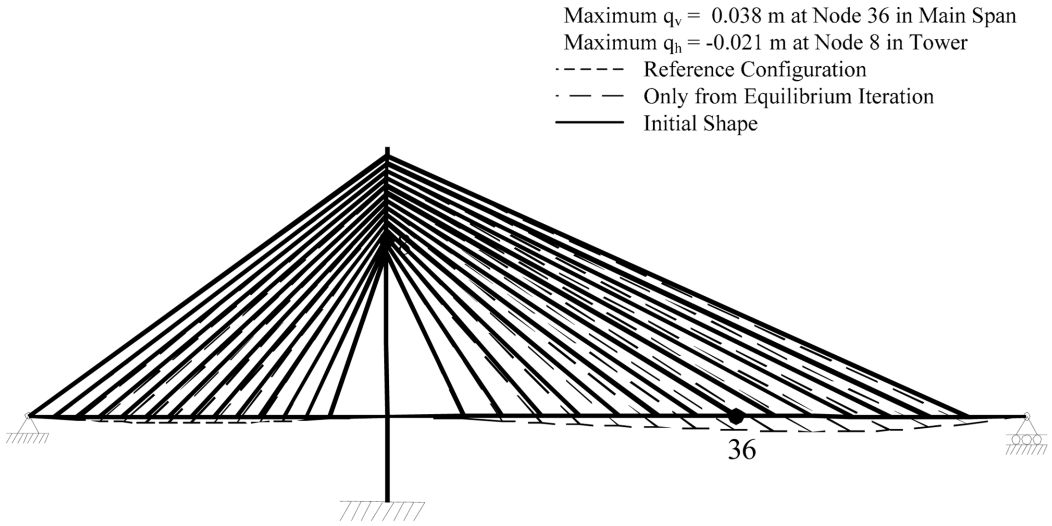

(a) OECS model

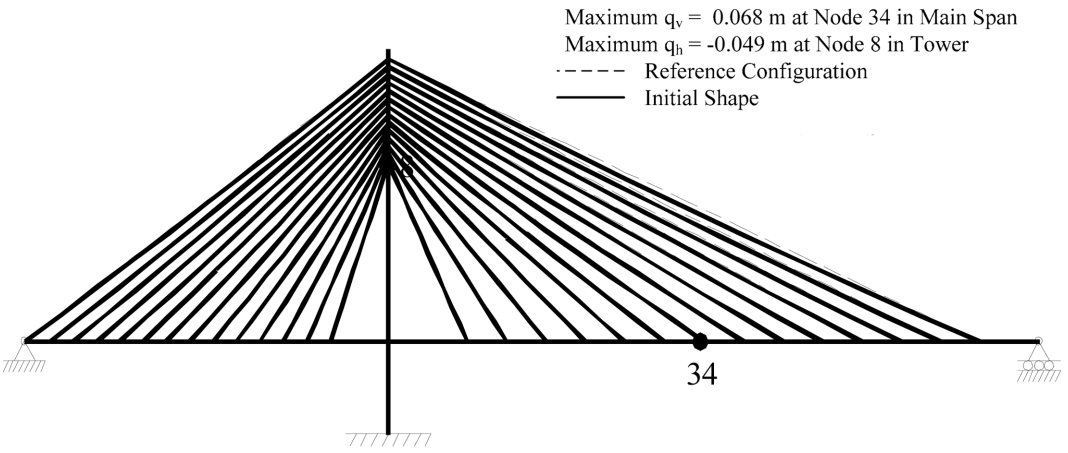

(b) MECS model

Fig. 6 Initial shapes of the Kao Ping Hsi Bridge

Kao Ping Hsi Bridge. In both Figs. 5(a) and 5(b), nodes 37, 38, 40, 45 and 46 are selected as the control points for checking the deck displacement in the vertical direction, while node 19 is chosen as the control point for checking the tower displacement in the horizontal direction. The convergence tolerance ε_r is set to 10^{-4} in this study.

Fig. 6(a) shows the initial shape of the OECS model of the Kao Ping Hsi Bridge (solid line), indicating that the maximum vertical and horizontal displacements measured from the reference configuration (short dashed line) are 0.038 m at node 36 in the main span of the deck and −0.021 m at node 8 in the tower, respectively. The shape of each stay cable represented by a single cable element is straight as expected. Fig. 6(a) also illustrates that the overall displacement obtained by the two-loop iteration method, i.e., the equilibrium and shape iterations, is comparatively smaller than that only from the equilibrium iteration (long dashed line). Consequently, the initial shape based on the two-loop iteration method appears to be able to appropriately describe the geometric configurations of cable-stayed bridges.

Fig. 6(b) shows the initial shape of the MECS model of the Kao Ping Hsi Bridge (solid line), indicating that the maximum vertical and horizontal displacements measured from the reference configuration (short dashed line) are 0.068 m at node 34 in the main span of the deck and −0.049 m at node 8 in the tower, respectively. The sagging shape occurs in the stay cables due to the fact that each stay cable is simulated by multiple cable elements.

4.2 Modal analysis and modal coupling assessment

According to the results of the initial shape analysis presented in Section 4.1, the modal analysis of the OECS and MECS models using the finite element computations developed in Section 2.4 are conducted to calculate the natural frequency and normalized mode shape of the individual modes of the Kao Ping Hsi Bridge. The modal coupling assessment based on the proposed formulas in Section 2.5 is also performed to obtain the generalized mass ratios among the structural components for each mode of such bridge. These results can be used to provide a variety of viewpoints to illustrate the mechanism of the deck-stay interaction with the appropriate initial shapes of cable-stayed bridges.

Table 1 summarizes the modal properties of the Kao Ping Hsi Bridge based on the OECS model (modes 1 to 3) and the MECS model (modes 1 to 24). In this table, f_n and $\overline{Y}_n$ represent the natural frequency and the normalized mode shape of the nth mode, respectively. As expected, the MECS model reveals the global, local and coupled modes, whereas the OECS model only yields the global modes. The modal properties of modes 1 and 2 in the OECS model are individually similar to those of modes 1 and 12 in the MECS model, because these modes represent the global modes. While mode 3 in the OECS model is identified as the global mode, mode 19 in the MECS model is the coupled mode. The other coupled mode can also be observed in mode 18 in the MECS model. These results suggest that the interaction between the deck-tower system and stay cables can be captured by the MECS model, but not by the OECS model. Also due to the limitations of the OECS model, modes 2 to 11, modes 13 to 17 and modes 20 to 24, which represent the local modes of the stay cables, are successfully captured by the MECS model, but not by the OECS model.

Fig. 7 shows the relationship between the natural frequency and the mode number for the first 24 modes of the MECS model of the Kao Ping Hsi Bridge. For reference, the fundamental frequency of stay S19 (0.6908 Hz) is also included. This frequency is calculated based on the assumption that stay S19 is clamped at both ends (Irvine 1981).

Table 1 Comparisons between corresponding modal properties of the OECS and MECS models of the Kao Ping Hsi Bridge

OECS				MECS			
n	f_n (Hz)	$\overline{Y}_n$	Type	n	f_n (Hz)	$\overline{Y}_n$	Type
1	0.2877	1st DT	G	1	0.3053	1st DT	G
				2	0.3382	1st S28	L
				3	0.3852	1st S27	L
				4	0.4274	1st S26	L
				5	0.4554	1st S1	L
				6	0.4653	1st S25	L
				7	0.4899	1st S24	L
				8	0.5067	1st S23	L
				9	0.5269	1st S22	L
				10	0.5378	1st S2	L
				11	0.5471	1st S21	L
2	0.5455	2nd DT	G	12	0.5686	2nd DT	G
				13	0.5944	1st S3	L
				14	0.6040	1st S20	L
				15	0.6333	1st S4	L
				16	0.6346	2nd S28	L
				17	0.6835	1st S5	L
				18	0.6850	3rd DT 1st S19	C
3	0.6854	3rd DT	G	19	0.7171	3rd DT 1st S19	C
				20	0.7269	1st S6	L
				21	0.7500	2nd S27	L
				22	0.7590	1st S7	L
				23	0.8008	1st S8	L
				24	0.8184	1st S18	L

DT: Deck-tower system
S: Stay cable
G: Global mode
L: Local mode
C: Coupled mode

Figs. 8(a) and 8(b) illustrate the normalized mode shapes of the individual modes of the OECS model (modes 1 to 3) and the MECS model (modes 1 to 24) of the Kao Ping Hsi Bridge, respectively. Each normalized mode shape (solid line) is measured from the initial shape (dashed

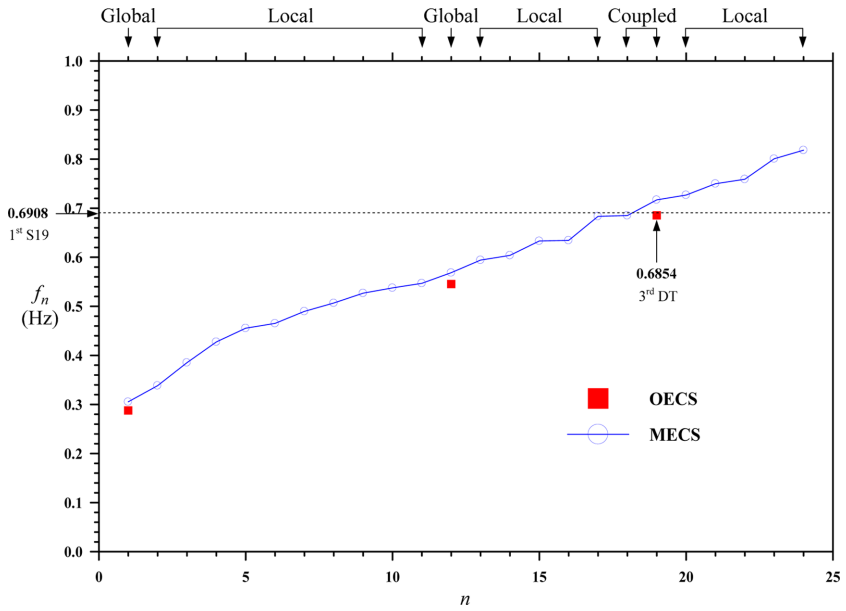

Fig. 7 Relationships between natural frequencies and mode numbers of the MECS model of the Kao Ping Hsi Bridge

line) obtained in Section 4.1.

To quantitatively assess the degree of coupling for each mode, Fig. 9 depicts the variations in the generalized mass ratios with respect to the mode number for the first 24 modes of the MECS model of the Kao Ping Hsi Bridge. In this figure, $\overline{M}_n^s, \overline{M}_n^d$ and $\overline{M}_n^t$ represent the generalized mass ratios of the stay cable, the deck and the tower of the nth mode, respectively. The sum of $\overline{M}_n^s, \overline{M}_n^d$ and $\overline{M}_n^t$ is 1 for the corresponding n ($n = 1$–24). It is evident that $\overline{M}_n^t$ ($n = 1$–24) approaches 0 for the first 24 modes due to the high rigidity of the concrete tower, resulting in the insignificant tower deformations in the lower modes sensitive to the ambient excitations, as can also be seen in Fig. 8(b). These results are in agreement with the literature (Gimsing 1997).

It can be seen in Table 1, Fig. 7, Figs. 8(a) and 8(b) that for the global modes, f_n and $\overline{Y}_n$ ($n = 1, 2$) in the OECS model are individually similar to f_n and $\overline{Y}_n$ ($n = 1, 12$) in the MECS model. It is consistent with the results in Fig. 9 that for modes 1 and 12 in the MECS model, the sum of $\overline{M}_n^d$ and $\overline{M}_n^t$ ($n = 1, 12$) is close to 0.9, whereas $\overline{M}_n^s$ ($n = 1, 12$) approaches 0.1. Consequently, these modes are primarily dominated by the deformations of the deck-tower system with the quasi-static motions of the stay cables. This type of response can be identified as the "pure" deck mode in the analytical model (Liu *et al.* 2005).

It also can be seen in Fig. 9 that for modes 2 to 11, modes 13 to 17 and modes 20 to 24 in the MECS model, $\overline{M}_n^s$ ($n = 2-11, 13-17, 20-24$) is close to 1, whereas the sum of $\overline{M}_n^d$ and $\overline{M}_n^t$ ($n = 2-11, 13-17, 20-24$) approaches 0. It is consistent with the results in Table 1, Fig. 7 and Fig. 8(b) that $\overline{Y}_n$ ($n = 2-11, 13-17, 20-24$) in the MECS model is the local mode predominantly consisting of the stay cable motions with negligible deformations of the deck-tower system. This type of response can be recognized as the "pure" cable mode in the analytical model (Liu *et al.* 2005).

As shown in Table 1, Fig. 7, Figs. 8(a) and 8(b), the difference between f_{19} in the MECS model

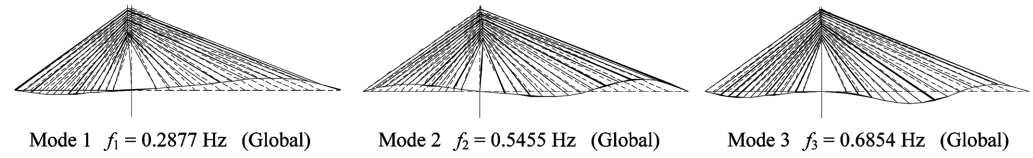

(a) OECS model

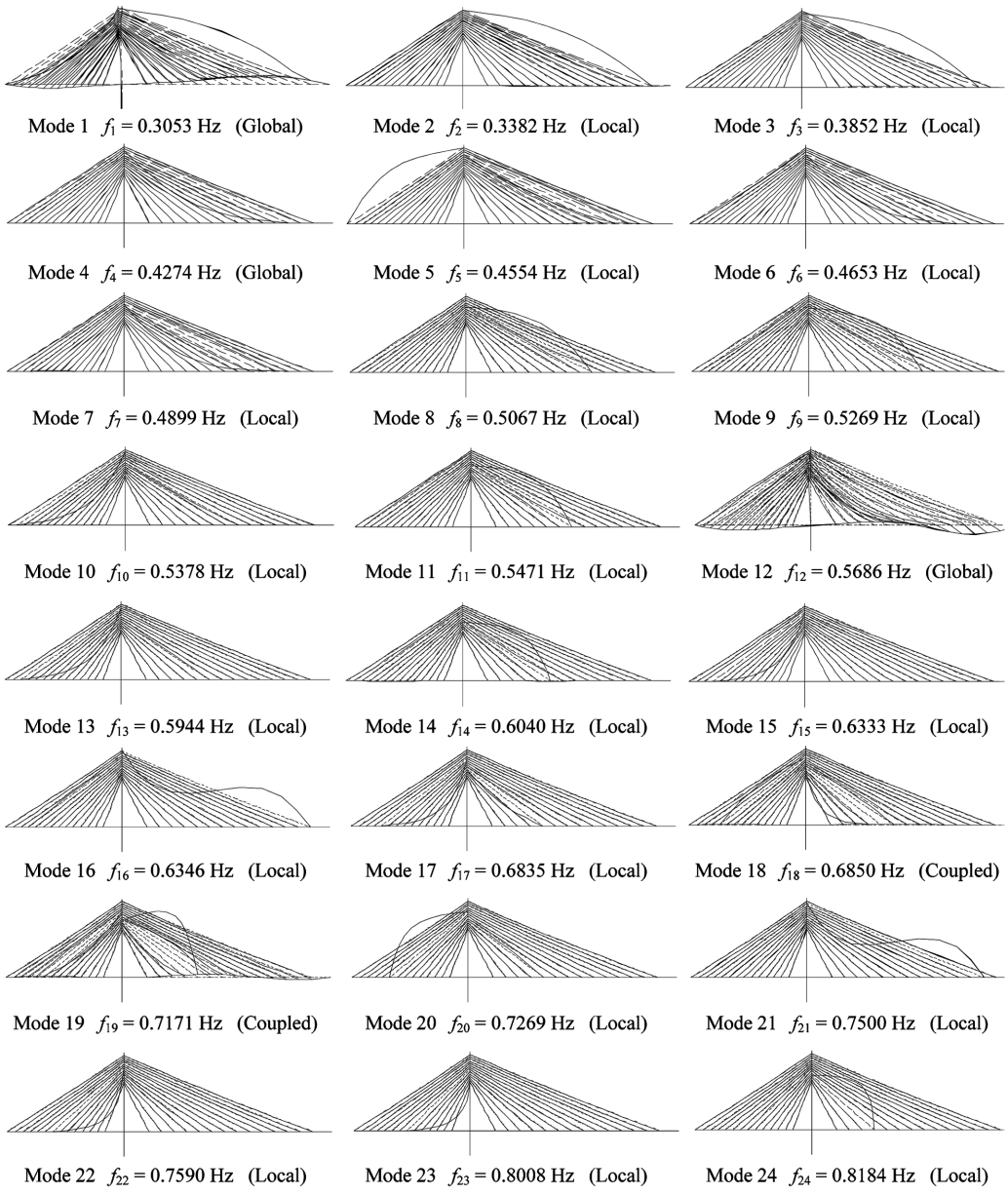

(b) MECS model

Fig. 8 Normalized mode shapes of the Kao Ping Hsi Bridge

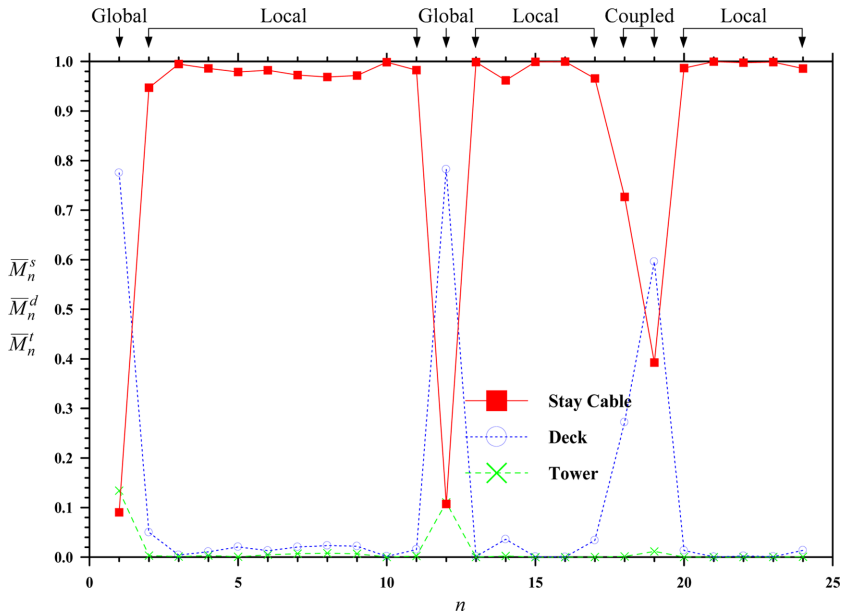

Fig. 9 Variations in generalized mass ratios with respect to mode numbers of the MECS model of the Kao Ping Hsi Bridge

(0.7171 Hz) and f_3 in the OECS model (0.6854 Hz) is evident due to the fact that $\overline{Y}_{19}$ in the MECS model is the coupled mode, but $\overline{Y}_3$ in the OECS model is the global mode, i.e., the "pure" deck-tower mode. Similarly, f_{18} in the MECS model (0.6850 Hz) branches from the fundamental frequency of stay S19 clamped at both ends (0.6908 Hz). This is because $\overline{Y}_{18}$ in the MECS model is the coupled mode, while the fundamental mode shape of stay S19 can be regarded as the "pure" stay cable mode. These observations are attributed to the frequency loci veering when the natural frequency of the "pure" deck-tower mode (0.6854 Hz) approaches that of the "pure" stay cable mode (0.6908 Hz). As illustrated in Fig. 9, the sum of $\overline{M}_{19}^d$ and $\overline{M}_{19}^t$ is relatively higher than $\overline{M}_{19}^s$, whereas the sum of $\overline{M}_{18}^d$ and $\overline{M}_{18}^t$ is comparatively lower than $\overline{M}_{18}^s$. Consequently, $\overline{Y}_{18}$ and $\overline{Y}_{19}$ in the MECS model are the pair of coupled modes with the similar configurations, which have substantial contributions from both the deck-tower system and stay cables. These phenomena correspond to the mode localization. This type of response coincides with the coupled mode in the analytical model (Liu *et al.* 2005).

In summary, the coupled modes are attributed to the frequency loci veering and mode localization when the "pure" deck-tower frequency and the "pure" stay cable frequency approach one another, implying that the mode shapes of such coupled modes are simply different from those of the deck-tower system or stay cables alone. The distribution of the generalized mass ratios between the deck-tower system and stay cables are useful indices for quantitatively assessing the degree of coupling for each mode. These results are demonstrated to fully understand the mechanism of the deck-stay interaction with the appropriate initial shapes of cable-stayed bridges.

5. Conclusions

This paper has provided a variety of viewpoints to illustrate the mechanism of the deck-stay interaction with the appropriate initial shapes of cable-stayed bridges. Based on the smooth and convergent bridge shapes obtained by the initial shape analysis, the OECS and MECS models of the Kao Ping Hsi Bridge are developed to verify the applicability of the analytical model and numerical formulation from the field observations in the authors' previous work. For this purpose, the modal analysis of the two finite element models are conducted to calculate the natural frequency and normalized mode shape of the individual modes of the bridge. The modal coupling assessment is also performed to obtain the generalized mass ratios among the structural components for each mode of the bridge.

The findings indicate that the coupled modes are attributed to the frequency loci veering and mode localization when the "pure" deck-tower frequency and the "pure" stay cable frequency approach one another, implying that the mode shapes of such coupled modes are simply different from those of the deck-tower system or stay cables alone. The distribution of the generalized mass ratios between the deck-tower system and stay cables are useful indices for quantitatively assessing the degree of coupling for each mode. These results are demonstrated to fully understand the mechanism of the deck-stay interaction with the appropriate initial shapes of cable-stayed bridges.

References

Abdel-Ghaffar, A.M. and Khalifa, M.A. (1991), "Importance of cable vibration in dynamics of cable-stayed bridges", *J. Eng. Mech., ASCE*, **117**(11), 2571-2589.

Au, F.T.K., Cheng, Y.S., Cheung, Y.K. and Zheng, D.Y. (2001), "On the determination of natural frequencies and mode shapes of cable-stayed bridges", *Appl. Math. Model.*, **25**(12), 1099-1115.

Caetano, E., Cunha, A. and Taylor, C.A. (2000a), "Investigation of dynamic cable-deck interaction in a physical model of a cable-stayed bridge. Part I: modal analysis", *Earthq. Eng. Structu. D.*, **29**(4), 481-498.

Caetano, E., Cunha, A. and Taylor, C.A. (2000b), "Investigation of dynamic cable-deck interaction in a physical model of a cable-stayed bridge. Part II: seismic response", *Earthq. Eng. Structu. D.*, **29**(4), 499-521.

Caetano, E., Cunha, A., Gattulli, V. and Lepidi, M. (2008), "Cable-deck dynamic interactions at the International Guadiana Bridge: On-site measurements and finite element modelling", *Struct. Control Hlth. Monit.,* **15**(3), 237-264.

Cheng, W.L. (2001), *Kao Ping Hsi Bridge*, Taiwan Area National Expressway Engineering Bureau, Ministry of Transportation and Communications, Taipei, Taiwan.

Ernst, H.J. (1965), "Der E-modul von Seilen unter Berücksichtigung des Durchhanges", *Der Bauingenieur*, **40**(2), 52-55. (in German)

Fleming, J.F. (1979), "Nonlinear static analysis of cable-stayed bridge structures", *Comput. Struct.*, **10**(4), 621-635.

Fujino, Y., Warnitchai, P. and Pacheco, B.M. (1993), "An experimental and analytical study of autoparametric resonance in a 3DOF model of cable-stayed-beam", *Nonlin. Dyn.*, **4**(2), 111-138.

Gattulli, V. and Lepidi, M. (2003), "Nonlinear interactions in the planar dynamics of cable-stayed beam", *Int. J. Solids Struct.*, **40**(18), 4729-4748.

Gattulli, V. and Lepidi, M. (2007), "Localization and veering in the dynamics of cable-stayed bridges", *Comput. Struct.*, **85**(21-22), 1661-1678.

Gattulli, V., Lepidi, M., Macdonald, J.H.G. and Taylor, C.A. (2005), "One-to-two global-local interaction in a cable-stayed beam observed through analytical, finite element and experimental models", *Int. J. Nonlin. Mech.*, **40**(4), 571-588.

Gattulli, V., Morandini, M. and Paolone, A. (2002), "A parametric analytical model for non-linear dynamics in

cable-stayed beam", *Earthq. Eng. Struct. D.*, **31**(6), 1281-1300.
Gimsing, N.J. (1997), *Cable Supported Bridges: Concept and Design*, Second Edition, John Wiley & Sons, Ltd, Chichester, UK.
Irvine, H.M. (1981), *Cable Structures*, MIT Press, Cambridge, Massachusetts, USA.
Lilien, J.L. and Pinto da Costa, A. (1994), "Vibration amplitudes caused by parametric excitation of cable stayed structures", *J. Sound Vib.*, **174**(1), 69-90.
Liu, M.Y., Lin, L.C. and Wang, P.H. (2011), "Dynamic characteristics of the Kao Ping Hsi Bridge under seismic loading with focus on cable simulation", *Int. J. Struct. Stab. Dyn.*, **11**(6), 1179-1199.
Liu, M.Y., Zuo, D. and Jones, N.P. (2005), "Deck-induced stay cable vibrations: Field observations and analytical model", *Proceedings of the Sixth International Symposium on Cable Dynamics*, Charleston, South Carolina, September.
Pinto da Costa, A., Martins, J.A.C., Branco, F. and Lilien, J.L. (1996), "Oscillations of bridge stay cables induced by periodic motions of deck and/or towers", *J. Eng. Mech.*, *ASCE*, **122**(7), 613-622.
Tuladhar, R., Dilger, W.H. and Elbadry, M.M. (1995), "Influence of cable vibration on seismic response of cable-stayed bridges", *Can. J. Civil Eng.*, **22**(5), 1001-1020.
Wang, P.H. and Yang, C.G. (1996), "Parametric studies on cable-stayed bridges", *Comput. Struct.*, **60**(2), 243-260.
Wang, P.H., Lin, H.T. and Tang, T.Y. (2002), "Study on nonlinear analysis of a highly redundant cable-stayed bridge", *Comput. Struct.*, **80**(2), 165-182.
Wang, P.H., Liu, M.Y., Huang, Y.T. and Lin, L.C. (2010), "Influence of lateral motion of cable stays on cable-stayed bridges", *Struct. Eng. Mech.*, **34**(6), 719-738.
Wang, P.H., Tang, T.Y. and Zheng, H.N. (2004), "Analysis of cable-stayed bridges during construction by cantilever methods", *Comput. Struct.*, **82**(4-5), 329-346.
Wang, P.H., Tseng, T.C. and Yang, C.G. (1993), "Initial shape of cable-stayed bridges", *Comput. Struct.*, **46**(6), 1095-1106.
Warnitchai, P., Fujino, Y. and Susumpow, T. (1995), "A non-linear dynamic model for cables and its application to a cable-structure system", *J. Sound Vib.*, **187**(4), 695-712.
Warnitchai, P., Fujino, Y., Pacheco, B.M. and Agret, R. (1993), "An experimental study on active tendon control of cable-stayed bridges", *Earthq. Eng. Structu. D.*, **22**(2), 93-111.